Ensemble of Local Texture Descriptor for Accurate Breast Cancer Detection from Histopathologic Images

Naaman Omar

Abstract—**Histopathological analysis is important for detection of the breast cancer (BC). Computer-aided diagnosis and detection systems are developed to assist the radiologist in the diagnosis process and to relieve the patient from unnecessary pain. In this study, a computer-aided diagnosis system for the early detection of benign and malignant breast cancer is proposed. The proposed system consists of feature extraction, feature ensemble, and classification stages. Various preprocessing steps such as grayscale conversion, noise filtering, and image resizing are employed on the input histopathological images. The local texture descriptors namely Local Binary Pattern (LBP), Frequency Decoded LBP (FDLBP), Binary Gabor Pattern (BGP), Local Phase Quantization (LPQ), Binarized Statistical Image Features (BSIF), CENsus TRansform hISTogram (CENTRIST), and Pyramid Histogram of Oriented Gradients (PHOG) are employed for feature extraction from the histopathologic images. The obtained features are then concatenated for the construction of the ensemble of the features. Three classifiers namely Support Vector Machines (SVM), K-nearest neighbor (KNN), and Neural Networks (NN) are used in the detection of the BC and the classification accuracy score is used for performance evaluation. A dataset called BreaKHis is used in the studies. There are 9109 microscopic pictures in BreaKHis, with 2480 benign samples and 5429 malignant samples. During the collection of the data, 82 patients' breast tumor tissues were envisioned using various magnification factors such as 40X, 100X, 200X, and 400X. The accuracy score is used to assess the acquired findings. The results show that the proposed method has the potential to use accurate BC detection.**

Keywords—**Histopathologic images, breast cancer, local texture descriptors, classifiers.**

I. INTRODUCTION

Breast cancer (BC) is a malignant tumor that starts with the uncontrolled proliferation of cells in any part of the breast and in which normal cells are damaged [1]. BC is the most common type of cancer in women and ranks second in cancer-related death rates after lung cancer. Many BC patients die each year due to late diagnosis and treatment. Therefore, early diagnosis and treatment of cancer are extremely important. There are many imaging techniques for the early diagnosis of BC. These are Contrast-Enhanced digital mammography,

ultrasound and magnetic resonance (MR) imaging, computed tomography (CT), and Positron Emission Tomography (PET) [2]. Although the initial detection of BC can be performed using these techniques, they do not guarantee that the abnormality detected in the breast tissues is malignant. Histopathology aims to differentiate between normal tissue, benign, and malignant cells. Histopathological analyzes have some disadvantages such as zooming, focusing and, panning needed on the image because it is very time-consuming depending on the experience, fatigue and, attention of the pathologists. Computer-assisted diagnosis (CAD) systems have been developed to accurately detect the mass removed from the breast and assist the physician. There are many studies in this field in the literature [3]-[10].

Deniz et al. used the deep transfer learning method for efficient BC detection in histopathological images. The pre-trained AlexNet CNN model was used in the work and the related accuracy scores were represented [3]. The authors used the fc6 and fc7 layers of the AlexNet model for feature extraction and the SVM classifier was used for the section of the BC. Selvathi et al. utilized an unsupervised deep learning approach with mammography. Dense mammography pictures were categorized using the approach. The accuracy percentage was determined to be 98.5 percent [4]. Geras et al. [5] used 886 thousand large-scale mammography images, where these images were utilized in a BC screening. A multi-deep convolutional network structure was employed in the research. It has been discovered that as the training set grows, so the performance also increases. The optimal resolution settings are the original resolution values. For cancer diagnosis, Bayramoglu et al. presented two alternative network topologies [6]. Convolutional neural networks were supposed to be used to categorize them. CNN was used to forecast malignant tumors as a single job. Spanhol et al. made a publicly accessible collection of 7909 BC histopathology images obtained from 82 individuals [7]. Both benign and cancerous images were included in the collection. The objective connected with this dataset was to automatically classify these images into two categories, which would be a useful computer-aided diagnosis tool for clinicians. Hameed et al. [8] developed an ensemble deep learning technique for the definitive categorization of BC histopathology pictures from non-carcinoma and carcinoma. The authors used pre-trained VGG16 and VGG19 architectures to train four distinct models. The study employed individual models, including fully-trained VGG16, fine-tuned VGG16, fully-trained VGG19, and fine-tuned VGG19. For the categorization of BC

histopathology images, a deep active learning architecture was developed to optimize learning accuracy with relatively minimal labeling [9]. The proposed technique entailed manually annotating the most useful unlabeled samples before including them in the training set. After that, the model was repeatedly updated with a growing training set. A novel histopathological image recognition technique was proposed by Guo et al. [10]. To combine more essential information in decision-making, the authors first built a hybrid Convolutional Neural Network (CNN) architecture based on GoogLeNet. Then, to decrease generalization error and enhance performance, a bagging approach and hierarchical voting tactic were proposed. Finally, to solve the constraints of the little amount of data, transfer learning and data augment techniques were used.

In this paper, an ensemble of local texture descriptors is used for efficient BC detection based on histopathological images. The input histopathological images are initially preprocessed for sake of convenience. To this end, noise removal and image resizing operations are employed. Then, LBP, Frequency Decoded LBP (FDLBP), Binary Gabor Pattern (BGP), Local Phase Quantization (LPQ), Binarized Statistical Image Features (BSIF), CENsus TRansform hISTogram (CENTRIST), and Pyramid Histogram of Oriented Gradients (PHOG) approaches are used for feature extraction from the histopathological images. Three classifiers namely SVM, kNN, and NN are used in the detection of the BC and the classification accuracy score is used for performance evaluation. In the experiments, a dataset namely the BreaKHis [7] is taken into account. BreaKHis has 9109 microscopic images, 2480 of which are benign and 5429 of which are malignant samples. 82 patients' breast tumor tissues were imagined using several magnifying factors such as 40X, 100X, 200X, and 400X throughout the gathering of the dataset. The contributions of this study are as follows;

1-) An ensemble of various texture descriptors is employed for efficient breast cancer detection.

2-) The results show that the proposed method produced comparable results with deep architectures where more computation time is needed.

The remainder of this paper is as follows. In the next section, the proposed method and the related theories are given. In Section III, the experimental works and the results are represented. The paper is concluded in Section IV.

II. PROPOSED METHOD

The illustration of the proposed method is given in figure 1. As seen in figure 1, the input to the proposed method is the histopathologic images. Image filtering and resizing operations are applied to these images at the beginning of the proposed method. To this end, Low pass filtering is considered. And, the input images are resized to 227×227 dimensions. After preprocessing, seven local texture descriptors are employed for feature extraction from the preprocessed input images. These local texture descriptors are LBP, FDLBP, BGP, LPQ, BSIF, CENTRIST, and PHOG, respectively. LBP effectively summarizes image local structures by comparing each pixel to its neighbors. FDLBP

enhances LBP by applying the multi-channel decoded LBP decoder idea to multi-frequency patterns. BGP was created to combine the benefits of Gabor filters and LBP. The Fourier transform phase in the immediate neighbors of a particular pixel was quantized to create LPQ.
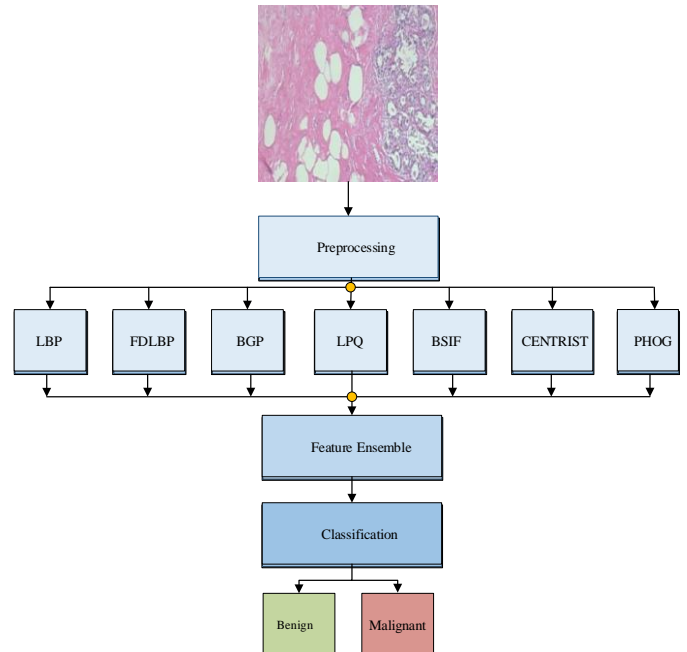

Fig. 1. The illustration of the proposed method

As a result, a strong framework was created to distinguish between blurred and low-resolution pictures. Binarization of responses to linear filters learned from natural pictures and independent component analysis was used to create BSIF. CENTRIST was created in the same way as the LBP. The histogram was utilized as CENTRIST characteristics after coding the pixel values. PHOG was created to encode a picture using its local form at multiple sizes while spreading the intensity and edge directions. The obtained local texture descriptors are then concatenated for obtaining the final feature vector. Three classifiers namely SVM, kNN, and NN are used in the classification stage of the proposed method. These classifiers are selected due to their high performance in machine learning applications. The obtained results are evaluated by using the classification accuracy metric.

A. LBP

The original LBP was developed by Ahonen et al. [11] to explain the spatial organization of local image textures. The LBP operator encodes an image's pixels by thresholding each pixel's neighborhood with the value of the center pixel and treating the result as a binary integer. The histogram is obtained as a feature set using the binary string.

B. FDLBP

Based on frequency decoders, Dubey et al. [12], [13] created the FDLBP face representation. The input images are first low-pass filtered, then high-pass filtered in the FDLBP

technique. Using the LBP operator on filtered images yields the LBP codes. Two encoders are given LBP binary codes to take advantage of the relationship between various frequency-filtered pictures. To build the FDLBP feature vector, a typical histogram technique is used for the output of decoders.

C. BGP

BGP was created by Zhang et al. [14] to combine the benefits of Gabor filters with LBP. BGP uses the difference between image regions instead of the difference between two pixels, like in LBP, to produce features resistant to noise. Gabor filters are used to calculate the difference between areas. The BGP feature descriptor is calculated by first using a filter bank to convolve in the image. To create a binarized vector, the resulting convoluted responses are thresholded based on the negative or positive sign. Then, utilizing orientations, the n-binary representation at the pixel is transformed into an integer value.

D. LPQ

Since it is retrieved by quantizing the Fourier transform phase in small areas, Ojansivu et al. [15] introduced LPQ that is resistant to blur and poor resolution.

E. BSIF

Kannala et al.[16] developed BSIF using independent component analysis and binarization of responses to linear filters learned from real pictures. The learned filters are used to encode each pixel as a binary string, which is then used to produce a BSIF descriptor for the histogram. The three phases of BSIF are mean subtraction of patches, principal component analysis to reduce dimensionality, and independent component analysis to compute statistically independent filters.

F. CENTRIST

CENTRIST [17] is based on the Census Transform, which compares the pixel value to its eight adjacent pixels and sets a bit 1 in the appropriate location if the center pixel's intensity value is greater than its given neighbor, otherwise 0. Every pixel's 8-bit binary string is then converted to a base-10 integer between 0 and 255.

G. PHOG

With the help of the distribution of the direction of intensity and edges, PHOG encodes pictures using its local form at various sizes [18]. The image is first subjected to a Canny edge detector, after which it is tessellated into smaller cells based on the number of levels. The PHOG descriptor is generated from the histograms of the occurrences of gradient orientations in these cells.

H. SVM

In the classification of linear and nonlinear two-class datasets, SVM is a classification method that seeks to locate the hyperplane that defines the border dividing class members from non-members. SVM is a supervised machine learning

method created by Vapnik and Cortes [19] in 1995 for both classification and regression tasks. The linear separation of positive and negative samples can be handled using Equation 1;

$$f(x) = w^T x + b = 0 \qquad (1)$$

where w indicates the weight vector and b is bias value used to determine the position of the hyperplane. A kernel trick is employed to transfer the input data to another hyperplane where the data is more convenient for linear separation. The best hyperplane can be determined using

$$\begin{cases} min\dfrac{\|w\|^2}{2} \\ y_i(w^T x_i + b) \geq 1 \quad i = 1,2,\dots,M \end{cases} \qquad (2)$$

I. KNN

KNN is a non-parametric and supervised data classification approach that is straightforward to use and develop [20]. To calculate the similarities between test and training samples, KNN employs a distance function. The test sample labels are then chosen using a majority vote process. Each test sample label is determined by the labels of its k nearest training samples which have high similarity with that test sample. The algorithm of the KNN approach is as follows;

> 1-) *Initialize the number of neighbors, K*
> 2-) *for each sample;*
>   2-1) *Calculate the distance between the query sample and the current sample.*
>   2-2) *Add the distance and index of the sample to an ordered collection.*
> 3-) *Sort the distances in ascending order.*
> 4-) *Pick the first K entries from the sorted collection.*
> 5-) *Get the labels of the selected K entries.*

J. NN

A NN is made up of artificial neurons, which are a collection of linked units or nodes that loosely resemble the neurons in a biological brain [21]-[23]. Each link may send a signal to other neurons, just like synapses in a human brain. An artificial neuron receives a signal, analyzes it, and then sends signals to the neurons it is linked. Edges are the terms for the connections. The weight of neurons and edges is generally adjusted as learning progresses. The signal strength at a connection is increased or decreased by the weight. Neurons may have a threshold that allows them to send a signal only if the aggregate signal exceeds it. Neurons are usually grouped into layers. On their inputs, various layers may apply different transformations. Signals pass from the first layer (input layer) to the last layer (output layer), perhaps several times. The output of a neuron in NN is given in

$$y = f(w^T x + b) \qquad (3)$$

where y is the output, x is the input and *w* indicates the weight vector and *b* is bias values, respectively.

III. EXPERIMENTAL WORKS AND RESULTS

The BreaKHis dataset [7] was utilized in experimental investigations because the suggested technique attempts to identify BC from histopathology pictures efficiently. Microscopic biopsy images of benign and malignant breast cancers are included in the collection. Specimens were obtained using an open surgical biopsy procedure. There are 7909 microscopic images in the BreaKHis collection, 2480 of which are benign and 5429 of which are malignant. Breast tumor samples from 82 individuals were collected utilizing several magnification factors such as 40X, 100X, 200X, and 400X during the collection of the dataset. All images are in color and have 700×460 pixels. The dataset was organized into five sections (Fold1, Fold2, Fold3, Fold4, and Fold5). In each fold, the dataset was divided into training and test set images. Fig. 2 shows some example images of benign and malignant breast tissues. While the first row of Fig. 2 shows the benign example images, the second row of Fig. 2 shows the malignant sample images.
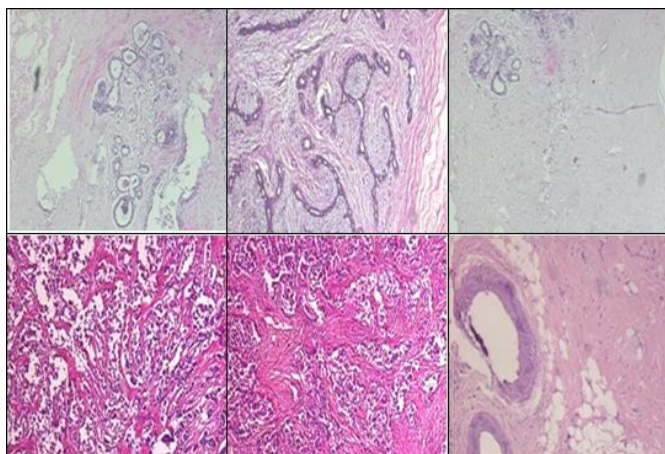

Fig. 2. The illustration of the proposed method

The color images were converted to grayscale images and low-pass filtered. Then each grayscale image was resized to 227×227. LBP, FDLBP, BGP, LPQ, BSIF, CENTRIST, and PHOG methods produced 59, 216, 4096, 254, 680, 256, and 4096-dimensional feature vectors, respectively. Thus, after the featured ensemble, a 9657-dimensional input feature vector was obtained. The SVM classifier with homogenous mapping and LIBLINEAR library with the L2-regularised L2-loss dual solver was considered because of their robustness to smaller amounts of training data [3]. The SVM parameter C is searched in the range of $[10^{-4}\text{-}10^3]$. The K value was chosen as 10 for KNN classifier. One hidden layered NN model was considered for NN classifier and the number of neurons was selected as 20. These values were determined by the trial and error approach.

The obtained accuracy scores for SVM, KNN, and NN were given in Tables I, II, and III, respectively. As seen in Table I, the SVM classifier achieved its best accuracy score for the 40X magnification factor and Fold1 part, where the accuracy score was 86.9%. In addition, the best achievement was

obtained for the 40X magnification factor, where the average accuracy score was 85.8%. An 84.2% average accuracy score was obtained for Fold 1 when the SVM classifier was considered.

TABLE I
THE ACHIEVEMENT OF THE SVM CLASSIFIER

	40X	100X	200X	400X	AVERAGE
FOLD1	86.9%	85.4%	84.7%	79.8%	84.2%
FOLD2	83.7%	85.2%	81.3%	77.1%	81.8%
FOLD3	86.7%	85.3%	79.9%	78.0%	82.5%
FOLD4	85.9%	86.1%	79.0%	77.8%	82.2%
FOLD5	85.8%	83.7%	80.4%	79.6%	82.3%
AVERAGE	85.8%	85.1%	81.1%	78.5%	82.6%

Table II represents the obtained achievements for the KNN classifier. Similar to the SVM achievement, the best accuracy score of 92.2% was produced for the 40X magnification factor and Fold1 part. Besides, the highest average accuracy scores of 88.5% and 84.9% were obtained for the 40X magnification factor and Fold 3 part, respectively.

TABLE II
THE ACHIEVEMENT OF THE KNN CLASSIFIER

	40X	100X	200X	400X	AVERAGE
FOLD1	92.2%	87.9%	82.7%	76.0%	84.7%
FOLD2	81.7%	86.0%	82.1%	78.9%	82.2%
FOLD3	91.8%	86.9%	80.9%	79.8%	84.9%
FOLD4	86.9%	85.3%	79.8%	75.4%	81.9%
FOLD5	90.0%	87.1%	81.4%	79.6%	84.5%
AVERAGE	88.5%	86.6%	81.4%	77.9%	83.6%

Lastly, Table III represents the achievements of the NN classifier. The best accuracy score of 90.2% was produced by the 40X magnification factor and Fold 4 part. The highest average accuracy score of s 89.1% and 86.4% were obtained for the 40X magnification factor and Fold 2 part, respectively. In addition, A 85.7% average classification accuracy score was obtained for the NN classifier, which was higher than the average achievements of the SVM and KNN classifiers.

TABLE III
THE ACHIEVEMENT OF THE NN CLASSIFIER

	40X	100X	200X	400X	AVERAGE
FOLD1	89.9%	89.4%	85.3%	78.7%	85.8%
FOLD2	88.7%	88.6%	84.6%	83.5%	86.4%
FOLD3	89.0%	87.7%	83.5%	80.0%	85.1%
FOLD4	90.2%	88.1%	84.0%	80.4%	85.7%
FOLD5	87.6%	86.9%	86.1%	82.6%	85.8%
AVERAGE	89.1%	88.1%	84.7%	81.0%	85.7%

In Table IV, we compared the achievement of the proposed method with some of the existing methods from the literature. In [7], the authors used various classifiers for BC detection. In [3], Deniz et al. used deep transfer learning for BC classification. As seen in Table 4, the proposed method produced better results than the results that were obtained in [7]. However, Deniz et al.'s achievements were better than the proposed method. Budak et al. [25] obtained 95.7%, 93.6%, 96.3% and 94.3% accuracy scores for 40X, 100X, 200X and 400X classes, respectively.

TABLE IV
THE PERFORMANCE COMPARISON OF THE PROPOSED METHOD WITH OTHER METHODS

METHODS	ACCURACY			
	40X	100X	200X	400X
SPANHOL ET AL. [7]	80.9%	80.7%	81.5%	79.4%
DENIZ ET AL. [3]	90.9%	90.6%	91.4%	91.3%
SPANHOL ET AL. [7]	81.6%	79.9%	85.1%	82.3%
BUDAK ET AL. [25]	95.7%	93.6%	96.3%	94.3%
PROPOSED	89.1%	88.1%	84.7%	81.0%

IV. CONCLUSION

In this paper, the ensemble of the local texture descriptors is used for BC discrimination. Various local texture descriptors are used in an ensemble way to obtain a final feature vector for efficient BC detection. From the experimental works, it is observed that the NN outperforms the SVM and KNN classifiers when the average accuracy scores are considered. Besides, it is observed that the 40X magnification factor generally produced better results than the other magnification factors for all classifiers. The experimental works revealed that the proposed method is quite convenient in the use of a support system for physicians. Although deep learning methods produce somewhat a bit better results than the proposed method, it can be said that the proposed method is more effective when the computational load and system complexity of the deep learning approaches are considered [24].

REFERENCES

[1] A. C. S. A. b. cancer., "https://www.cancer.org/content/dam/CRC/PDF/Public/8577.00.pdf".

[2] L. Wang, "Early diagnosis of breast cancer". Sensors. 2017;17–1572:1–20.," 2017.

[3] E. Deniz, A. Şengür, Z. Kadiroğlu, Y. Guo, V. Bajaj, and Ü. Budak, "Transfer learning based histopathologic image classification for breast cancer detection," Health information science and systems, vol. 6, pp. 1-7, 2018.

[4] A. P. D Selvathi, "Breast cancer detection ın mammogram ımages using deep learning technique," middle-east. J Sci Res. 2017;25(2):417–26., 2017.

[5] K. J. Geras, S. Wolfson, Y. Shen, N. Wu, S. Kim, E. Kim, et al., "High-resolution breast cancer screening with multi-view deep convolutional neural networks," arXiv preprint arXiv:1703.07047, 2017.

[6] N. Bayramoglu, J. Kannala, and J. Heikkilä, "Deep learning for magnification independent breast cancer histopathology image classification," in 2016 23rd International conference on pattern recognition (ICPR), 2016, pp. 2440-2445.

[7] F. A. Spanhol, L. S. Oliveira, C. Petitjean, and L. Heutte, "A dataset for breast cancer histopathological image classification," IEEE Transactions on Biomedical Engineering, vol. 63, pp. 1455-1462, 2015.

[8] Z. Hameed, S. Zahia, B. Garcia-Zapirain, J. Javier Aguirre, and A. María Vanegas, "Breast cancer histopathology image classification using an ensemble of deep learning models," Sensors, vol. 20, p. 4373, 2020.

[9] Q. Qi, Y. Li, J. Wang, H. Zheng, Y. Huang, X. Ding, et al., "Label-efficient breast cancer histopathological image classification," IEEE Journal of biomedical and health informatics, vol. 23, pp. 2108-2116, 2018.

[10] Y. Guo, H. Dong, F. Song, C. Zhu, and J. Liu, "Breast cancer histology image classification based on deep neural networks," in International Conference Image Analysis and Recognition, 2018, pp. 827-836.

[11] A. Hadid, M. Pietikainen, and T. Ahonen, "Face description with local binary patterns: Application to face recognition," IEEE Transactions on Pattern Analysis and Machine Intelligence, vol. 28, pp. 2037-2041, 2006.

[12] S. Ram Dubey, "Face Retrieval using Frequency Decoded Local Descriptor," arXiv e-prints, p. arXiv: 1709.06508, 2017.

[13] Z. Akhtar, and D. Dasgupta, "A comparative evaluation of local feature descriptors for deepfakes detection," in 2019 IEEE International Symposium on Technologies for Homeland Security (HST), 2019, pp. 1-5.

[14] L. Zhang, Z. Zhou, and H. Li, "Binary Gabor pattern: An efficient and robust descriptor for texture classification," in 2012 19Th IEEE international conference on image processing, 2012, pp. 81-84.

[15] V. Ojansivu and J. Heikkilä, "Blur insensitive texture classification using local phase quantization," in International conference on image and signal processing, 2008, pp. 236-243.

[16] J. Kannala and E. Rahtu, "Bsif: Binarized statistical image features," in Proceedings of the 21st international conference on pattern recognition (ICPR2012), 2012, pp. 1363-1366.

[17] J. Wu and J. M. Rehg, "Centrist: A visual descriptor for scene categorization," IEEE transactions on pattern analysis and machine intelligence, vol. 33, pp. 1489-1501, 2010.

[18] A. Bosch, A. Zisserman, and X. Munoz, "Representing shape with a spatial pyramid kernel," in Proceedings of the 6th ACM international conference on Image and video retrieval, 2007, pp. 401-408.

[19] C. Cortes and V. Vapnik, "Support-vector networks," Machine learning, vol. 20, pp. 273-297, 1995.

[20] D. Şengür and M. Turhan, "Prediction of the action identification levels of teachers based on organizational commitment and job satisfaction by using k-nearest neighbors method," Turkish Journal of Science and Technology, vol. 13, pp. 61-68, 2018.

[21] W. S. McCulloch and W. Pitts, "A logical calculus of the ideas immanent in nervous activity," The bulletin of mathematical biophysics, vol. 5, pp. 115-133, 1943.

[22] N. Omar, A. Sengur, and S. G. S. Al-Ali, "Cascaded deep learning-based efficient approach for license plate detection and recognition," Expert Systems with Applications, vol. 149, p. 113280, 2020.

[23] N. Omar, A. M. Abdulazeez, A. Sengur, and S. G. S. Al-Ali, "Fused faster RCNNs for efficient detection of the license plates," Indonesian Journal of Electrical Engineering and Computer Science, vol. 19, pp. 974-982, 2020.

[24] Y. Benhammou, B. Achchab, F. Herrera, and S. Tabik, "BreakHis based breast cancer automatic diagnosis using deep learning: Taxonomy, survey and insights". Neurocomputing, 375, 9-24, (2020).

[25] Ü. Budak, Z. Cömert, Z.N. Rashid, A. Şengür, M. Çıbuk, Computer-aided diagnosis system combining FCN and Bi-LSTM model for efficient breast cancer detection from histopathological images, Appl Soft Comput J, 85 (2019), p. 105765, 10.1016/j.asoc.2019.105765

Naaman O. Yaseen was born in Amedi City, Duhok, Iraq in 1981. He received the B.S. Duhok University 2004 and M.S. degrees in Zakho University 2011 in the college of science, computer science, in 2021 he received the Ph.D. degree in both (Duhok Polytechnic University and Firat University).

His current research program is in image processing, machine learning, and parallel processing. He is a member of IEEE, IEEE Cand computer and Communication Societies.